

Successful prenatal mannose treatment for congenital disorder of glycosylation-Ia in mice

Anette Schneider¹, Christian Thiel¹, Jan Rindermann², Charles DeRossi¹, Diana Popovici¹, Georg F Hoffmann¹, Hermann-Josef Gröne³ & Christian Körner¹

Congenital disorder of glycosylation-Ia (CDG-Ia, also known as PMM2-CDG) is caused by mutations in the gene that encodes phosphomannomutase 2 (PMM2, EC 5.4.2.8) leading to a multisystemic disease with severe psychomotor and mental retardation. In a hypomorphic Pmm2 mouse model, we were able to overcome embryonic lethality by feeding mannose to pregnant dams. The results underline the essential role of glycosylation in embryonic development and may open new treatment options for this disease.

PMM2 catalyzes the cytosolic conversion of mannose-6-phosphate to mannose-1-phosphate. Reduced PMM2 enzymatic activity leads to a decrease in the downstream products GDP-mannose and dolichol-P-mannose, which are key substrates in *N*-glycan biosynthesis. Smaller amounts of either substrate results in hypoglycosylation of glycoproteins, thereby causing CDG-Ia^{1,2}. In recent studies of a Pmm2 knockout mouse model for CDG-Ia, we found that complete loss of Pmm2 activity leads to embryonic lethality by 3.5 days post coitum (d.p.c.)³. As humans with CDG-Ia show a weak residual PMM2 activity, we generated two mouse lines harboring Pmm2-hypomorphic alleles—one containing an R137H mutation that is analogous to the R141H mutation found in human cases of CDG-Ia, and one containing an F118L mutation that is analogous to F122L, a synthetic mutation in the human protein that is predicted from X-ray crystallographic data⁴ to lead to a very mild loss of enzymatic activity (**Supplementary Fig. 1**).

We used heterozygous *Pmm2*^{+/^{R137H} and *Pmm2*^{+/^{F118L} mice to generate mice with the respective homozygous (*Pmm2*^{R137H/R137H} and *Pmm2*^{F118L/F118L}) or compound heterozygous (*Pmm2*^{R137H/F118L}) genotypes. In 95 analyzed mice arising from 13 matings of *Pmm2*^{+/^{R137H} parents, no *Pmm2*^{R137H/R137H} mice were recovered. Although we did not determine the specific time of death of the embryos, prenatal analysis from timed matings revealed the embryonic lethality to occur before 5.5-d.p.c. (data not shown). These observations are consistent with R141H homozygosity not being found in humans⁵. Furthermore, given that a recombinant human PMM2 protein with the R141H mutation shows no measurable enzymatic activity⁶, the early lethality of *Pmm2*^{R137H/R137H} embryos is comparable to that of Pmm2-null mice³.}}}

In contrast to *Pmm2*^{R137H/R137H} mice, *Pmm2*^{F118L/F118L} mice were viable, fertile and comparable in size and proportion to their wild-type siblings. They developed normally without any major phenotype up to adulthood. Histological examination of organs in 3- to 6-month-old mice and isoelectric focusing of serum transferrin (a glycoprotein used as marker in CDG diagnostics) did not yield any pathological findings (data not shown). Pmm activity (measured by an assay that does not differentiate between PMM1 and PMM2) in mouse embryonic fibroblasts (MEFs) cultivated from 9.5-d.p.c. *Pmm2*^{F118L/F118L} embryos was 42% (0.75 ± 0.19 pmol min⁻¹ per mg protein) of that of wild-type siblings (1.79 ± 0.38 pmol min⁻¹ per mg protein, $n = 7$, $P < 0.002$ (Student's *t* test)). Likewise, we found that Pmm activity was 38% of wild-type activity (0.22 ± 0.01 pmol min⁻¹ per mg protein in primary fibroblasts established from skin biopsies of 6-month-old homozygous mice compared to 0.58 ± 0.11 pmol min⁻¹ per mg protein in those from wild-type littermates, $n = 4$, $P < 0.007$ (Student's *t* test)). These results indicate that the residual Pmm2 activity in homozygous *Pmm2*^{F118L/F118L} mice is sufficient to prevent hypoglycosylation and subsequent pathological phenotypes.

Intercrossing *Pmm2*^{+/^{R137H} and *Pmm2*^{+/^{F118L} mice produced no viable *Pmm2*^{R137H/F118L} offspring (**Supplementary Table 1**), suggesting embryonic lethality associated with this genotype. To identify the day of embryonic death, we interrupted pregnancies at different time points and analyzed the embryos for their genotype and morphology. Between 7.5 d.p.c. and 9.5 d.p.c., *Pmm2*^{R137H/F118L} embryos showed progressive intrauterine growth retardation. At 9.5 d.p.c. (**Fig. 1a**), *Pmm2*^{+/⁺ embryos had a crown-rump length of 4.26 ± 0.50 mm, whereas *Pmm2*^{R137H/F118L} embryos had a crown-rump length of 2.73 ± 0.76 mm ($n = 6$; $P = 0.0014$ (Student's *t* test)). By 10.5 d.p.c., we detected only residues of *Pmm2*^{R137H/F118L} embryonic tissue and amniotic sacs, whereas *Pmm2*^{+/⁺ and heterozygous siblings developed normally (**Fig. 1a**). After 10.5 d.p.c., we could not identify any trace of *Pmm2*^{R137H/F118L} embryos (**Fig. 1a**; see **Supplementary Table 1**), localizing the time of death between 9.5 and 10.5 d.p.c.}}}}

Histological examination of 10.0-d.p.c. embryos revealed morphological defects in tissues from *Pmm2*^{R137H/F118L} embryos. In wild-type embryos, all embryonic and extraembryonic tissues were clearly identifiable (**Supplementary Fig. 2**), whereas in *Pmm2*^{R137H/F118L} embryos embryonic structures were difficult to identify owing to extensive degradation, as indicated by breakdown of myocardial tissues and reduction of compactness of the neural epithelium and the cephalic mesenchyme. The multiple organ degradation was accompanied by massive hemorrhaging within the extraembryonic supporting structures and potential loss of trophoblast giant cells (**Supplementary Fig. 2**). Nevertheless, whether the molecular defect underlying the termination of embryonic development results from a failure in the placenta or in the embryo itself is a topic for future investigations.

¹Center for Child and Adolescent Medicine and Center for Metabolic Diseases Heidelberg, Department Kinderheilkunde I, Heidelberg, Germany. ²Institut für Biochemie II, Göttingen, Germany. ³German Cancer Research Center Heidelberg, Division of Cellular and Molecular Pathology, Heidelberg, Germany. Correspondence should be addressed to C.K. (christian.koerner@med.uni-heidelberg.de).

Received 11 July; accepted 6 October; published online 11 December 2011; doi:10.1038/nm.2548

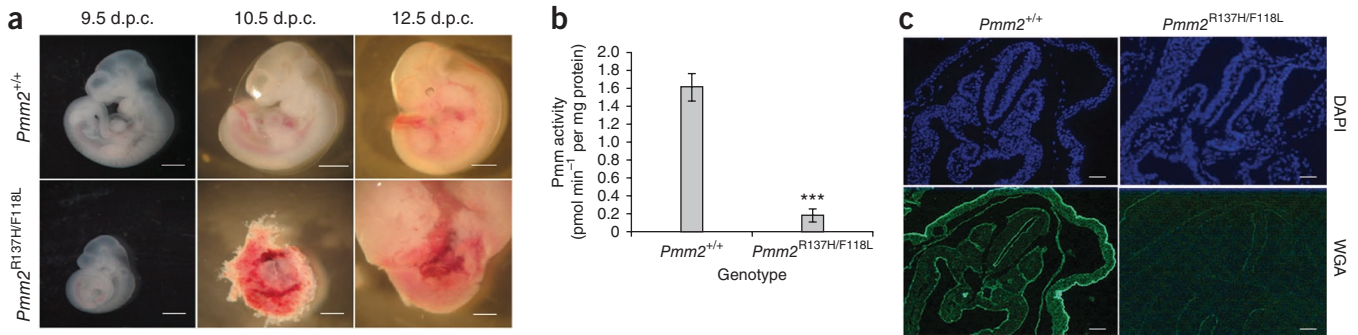


Figure 1 Microscopic, biochemical and histochemical examinations of *Pmm2*^{+/+} and *Pmm2*^{R137H/F118L} embryos. **(a)** Development of *Pmm2*^{+/+} and *Pmm2*^{R137H/F118L} embryos at 9.5, 10.5 and 12.5 d.p.c. Data are from six embryos of each genotype, arising from six separate littermates. Scale bars: 9.5 d.p.c., 1 mm; 10.5 d.p.c., 1.5 mm; 12.5 d.p.c., 2 mm. **(b)** Pmm activity, as measured in MEFs isolated at 9.5 d.p.c. from four *Pmm2*^{+/+} and four *Pmm2*^{R137H/F118L} embryos from four separate littermates. Enzyme activity is shown as the formation of mannose-1,6-bisphosphate in pmol min⁻¹ per mg protein. Error bars are s.e.m.; ****P* = 0.00018 (Student's *t* test). **(c)** DAPI nuclei and WGA staining of embryonic tissues at 9.5 d.p.c. Data are representative of 20 sections per embryo. Four mice of the respective genotype arising from four separate littermates were analyzed. Scale bars, 100 μm. Mouse procedures were approved by the regional council Karlsruhe (Department III) in Baden-Württemberg (Germany) and the University of Heidelberg (Germany). See **Supplementary Methods** for further technical information.

Enzymatic assays on MEFs isolated from embryos at 9.5 d.p.c. showed that Pmm activity of *Pmm2*^{R137H/F118L} mice was 11% of that measured in wild-type siblings (0.19 ± 0.07 pmol min⁻¹ mg per protein versus 1.61 ± 0.15 pmol min⁻¹ per mg protein, $n = 4$, $P = 0.00018$ (Student's *t* test)) (**Fig. 1b**), a level similar to that found in many humans with CDG-Ia. Lower Pmm2 activity leads to hypoglycosylation of glycoproteins in *Pmm2*^{R137H/F118L} embryos, as indicated in lectin binding studies with biotinylated wheat germ agglutinin (WGA) (detected by streptavidin-FITC), which identifies mature glycan structures (**Fig. 1c**). In *Pmm2*^{+/+} embryos, neural tube, neural epithelium of the neural lumen and cephalic vesicles, amniotic sac, amnion, myocardial tissue and the cephalic mesenchyme had strong fluorescence signals, whereas *Pmm2*^{R137H/F118L} embryos possessed substantially less fluorescence within these tissues (**Fig. 1c**). Taken together, these results indicate that *Pmm2*^{R137H/F118L} embryos have lower Pmm2 activity than wild-type littermates and this is associated with a general protein hypoglycosylation, resulting in embryonic lethality.

A promising concept for therapy for CDG-Ia is to counter the increased K_m requirements of mutated PMM2 by raising the intracellular substrate levels of mannose-6-phosphate by either oral or intravenous mannose supplementation. This would lead to higher levels of mannose-1-phosphate when metabolized by mutant forms of PMM2 with attenuated activity, an increase in production of GDP-mannose and dolichol-P-mannose and subsequent normalization of glycosylation. In fibroblasts derived from humans with CDG-Ia, we and others have shown that shortened glycan structures from lipid-linked oligosaccharides and newly synthesized glycoproteins were corrected by either addition of mannose to^{7,8} or reduction of glucose concentration in⁸ the cell culture medium. Nevertheless, neither oral administration of mannose to patients with CDG-Ia over a period of 6 months nor intravenous mannose supplementation for 3 weeks led to any measurable positive effect on coagulation abnormalities or altered isoelectric focusing patterns of serum transferrin, despite increased serum mannose concentrations^{9,10}.

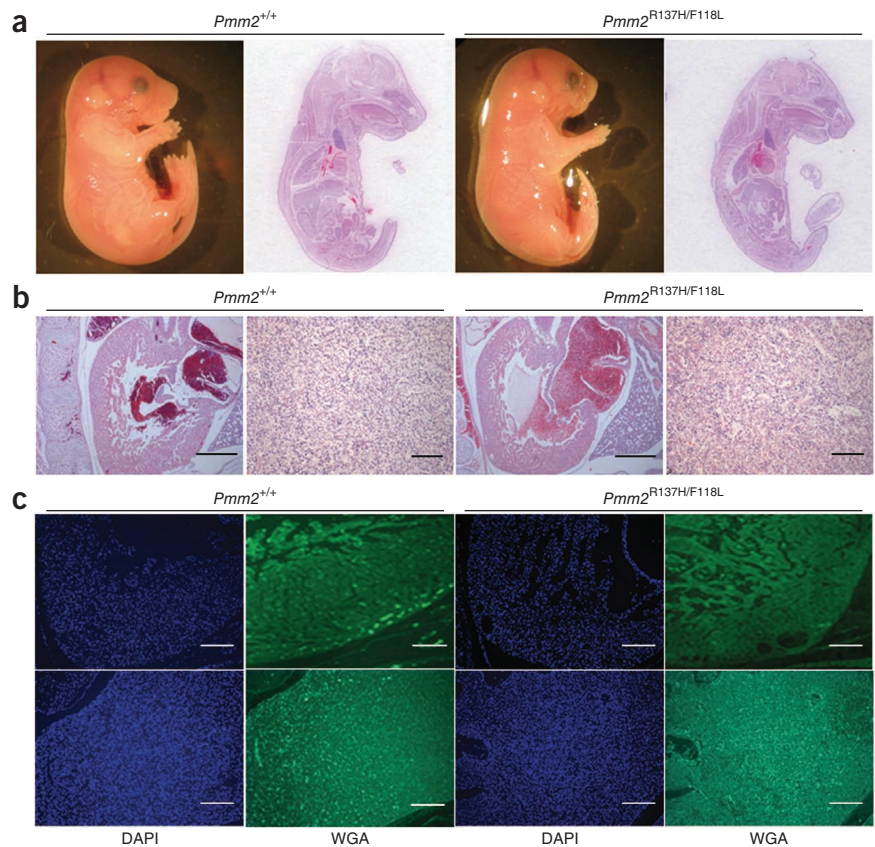
To determine whether mannose supplementation could correct the abnormal glycosylation and lethality in *Pmm2*^{R137H/F118L} embryos, we placed heterozygous *Pmm2*^{+/F118L} female mice on an oral mannose treatment protocol based on trials in humans with CDG-Ia^{10,11} (9 mg mannose per ml drinking water). We started the supplementation 1 week before mating to ensure that the mannose concentrations in

maternal blood, and therefore the embryonic exposure to mannose, would be stable throughout gestation, and maintained treatment until 16.5 d.p.c. or weaning. In comparison to untreated female *Pmm2*^{+/F118L} mice, mannose feeding led to almost twofold higher serum mannose concentrations in female *Pmm2*^{+/F118L} mice (81.66 ± 18.19 μM mannose, $n = 5$, versus 49.14 ± 12.55 μM mannose, $n = 10$, $P = 0.007$ (Student's *t* test); **Supplementary Fig. 3**).

Remarkably, mannose supplementation rescued *Pmm2*^{R137H/F118L} embryos and allowed them to survive beyond weaning (**Supplementary Table 2**). In contrast to *Pmm2*^{+/+} offspring, *Pmm2*^{R137H/F118L} offspring under mannose supplementation had high serum mannose concentrations (139.48 ± 52.96 μM mannose, $n = 9$, versus 81.77 ± 14.88 μM mannose, $n = 7$, $P = 0.0095$ (Student's *t* test)) (**Supplementary Fig. 3**). The substantially higher concentration of serum mannose in the treated mice presumably resulted from reduced mannose usage due to deficient Pmm2 enzyme activity. Histological examination of embryos at 16.5 d.p.c. revealed no differences in the morphology of heart, liver, lung, kidney, thymus, spleen and brain tissue between wild-type and *Pmm2*^{R137H/F118L} mice (**Fig. 2a,b** and data not shown). In addition, the glycosylation pattern monitored by WGA lectin histochemistry in these organs was comparable between *Pmm2*^{+/+} and *Pmm2*^{R137H/F118L} embryos (**Fig. 2c** and data not shown), indicating that there was mannose-mediated normalization of glycosylation. Isoelectric focusing of serum transferrin from 8-week-old mice of all genotypes revealed no differences in levels of glycosylation (data not shown). Pmm activity in compound heterozygous embryos ($n = 2$) rescued with mannose remained at approximately 11% that of wild-type embryos (data not shown), indicating that the mannose rescue was not a result of increased Pmm2 activity.

To investigate whether the pathological changes in *Pmm2*^{R137H/F118L} offspring occurred after termination of mannose supplementation, we reconverted dams to normal drinking water after weaning and maintained the pups on normal drinking water. After 4 months, we found the serum mannose concentration was comparable between *Pmm2*^{+/+} (65.50 ± 8.3 μM mannose, $n = 3$) and *Pmm2*^{R137H/F118L} (68.50 ± 16.6 μM mannose, $n = 4$, $P = 0.723$ (Student's *t* test)) littermates (**Supplementary Fig. 3**). There were no obvious behavioral or macroscopic alterations in phenotype in *Pmm2*^{R137H/F118L} offspring compared to wild-type siblings. Histological analyses of a variety of tissues, such as brain, heart, liver, lung, spleen and kidney, were

Figure 2 Histological and WGA lectin binding analyses of mannose-supplemented *Pmm2*^{+/+} and *Pmm2*^{R137H/F118L} embryos 16.5 d.p.c. Embryos were dissected and genotyped. Histological samples were fixed in 4% formaldehyde, embedded in paraffin and stained with H&E. (a) Stereomicroscopic pictures (left) and H&E staining (right) of central sagittal sections of whole *Pmm2*^{+/+} and *Pmm2*^{R137H/F118L} embryos. (b) H&E staining of the heart (left; scale bars: 500 μ m) and the liver (right; scale bars: 100 μ m) of *Pmm2*^{+/+} and *Pmm2*^{R137H/F118L} embryos, respectively. (c) DAPI nuclei (left) and WGA staining (right) of hearts (top) and livers (bottom) of *Pmm2*^{+/+} and *Pmm2*^{R137H/F118L} embryos, respectively (Scale bars, 200 μ m). In a–c, data are representative of four mice of the respective genotype arising from four separate littersmates. Twenty sections per embryo were analyzed by H&E and lectin staining.



similarly unremarkable (**Supplementary Fig. 4**), as was the glycosylation state of serum transferrin (data not shown).

Although identification of the specific cause for the *Pmm2*^{R137H/F118L} lethality is outside the scope of this report, we speculate that general hypoglycosylation of N-linked glycoproteins due to *Pmm2*^{R137H/F118L} deficiency has severe effects on a multitude of pathways involved in embryogenesis that may result in the observed fatal outcome. In our *Pmm2*^{R137H/F118L} mouse model, the elevation of the extracellular mannose concentration by the simple addition of mannose presumably leads to a higher uptake of sugar and, in turn, an increase in the intracellular GDP-mannose level, which is crucial for N-linked glycoprotein biosynthesis. Our results therefore suggest a central role for an increased glycosylation state and an elevated amount of N-linked glycoproteins during a specific time frame in embryonic development that, to our knowledge, has not been described so far.

Given that people with CDG-Ia are already in early childhood when they start mannose therapy, it is possible that essential developmental steps during embryogenesis and infancy may have already been negatively affected by hypoglycosylation, resulting in a CDG-Ia phenotype that is unresponsive to mannose treatment. Consistent with this hypothesis, it is known that the intrauterine environment during human gestation influences the development of disease, including metabolic disorders, later in life¹².

In light of the positive results achieved in this study, initiating a therapeutic mannose regimen before conception to women at risk for having descendants with CDG-Ia or after conception in the case of CDG-Ia confirmed *in utero* by early prenatal diagnosis may overcome impairment of key developmental steps that influence the postnatal development of the disease. This, in turn, could potentially lessen the severity of disabilities that afflict people with CDG-Ia or, ideally, could prevent the disease altogether.

METHODS

Methods and any associated references are available in the online version of the paper at <http://www.nature.com/naturemedicine/>.

Note: Supplementary information is available on the Nature Medicine website.

ACKNOWLEDGMENTS

The work of C.K. and C.T. was supported by grants of the Deutsche Forschungsgemeinschaft (KO 2152/3-2 and TH1461/2-1) and the Fritz Thyssen Stiftung. The work of C.D. was supported by a US National Institutes of Health grant (R21 HD062914) and The Rocket Fund.

AUTHOR CONTRIBUTIONS

A.S. and C.T. contributed equally, and were both responsible for experimental design, mouse experiments and data analysis, and they wrote the manuscript. J.R. generated mouse embryonic stem cell lines. C.D. and D.P. performed mouse dissections and histology. G.F.H. assisted in data analysis. H.-J.G. analyzed the histological data. C.K. supervised all aspects of this work, analyzed data and wrote the manuscript.

COMPETING FINANCIAL INTERESTS

The authors declare no competing financial interests.

Published at <http://www.nature.com/naturemedicine/>.

Reprints and permissions information is available at <http://www.nature.com/reprints/index.html>.

- Matthijs, G. *et al. Nat. Genet.* **16**, 88–92 (1997).
- Grünwald, S. *Biochim. Biophys. Acta* **1792**, 827–834 (2009).
- Thiel, C., Lübke, T., Matthijs, G., von Figura, K. & Körner, C. *Mol. Cell. Biol.* **26**, 5615–5620 (2006).
- Silvaggi, N.R. *et al. J. Biol. Chem.* **281**, 14918–14926 (2006).
- Matthijs, G., Schollen, E., Van Schaftingen, E., Cassiman, J.J. & Jaeken, J. *Am. J. Hum. Genet.* **62**, 542–550 (1998).
- Kjaergaard, S., Skovby, F. & Schwartz, M. *Eur. J. Hum. Genet.* **7**, 884–888 (1999).
- Panneerselvam, K. & Freeze, H.H. *J. Clin. Invest.* **97**, 1478–1487 (1996).
- Körner, C., Lehle, L. & von Figura, K. *Glycoconj. J.* **15**, 499–505 (1998).
- Mayatepek, E., Schröder, M., Kohlmüller, D., Bieger, W.P. & Nützenadel, W. *Acta Paediatr.* **86**, 1138–1140 (1997).
- Mayatepek, E. & Kohlmüller, D. *Eur. J. Pediatr.* **157**, 605–606 (1998).
- Kjaergaard, S. *et al. Acta Paediatr.* **87**, 884–888 (1998).
- Godfrey, K.M. & Barker, D.J.P. *Am. J. Clin. Nutr.* **71**, 1344S–1352S (2000).